Heliyon 5 (2019) e02869

Contents lists available at ScienceDirect

Heliyon

journal homepage: www.heliyon.com

Research article

Grb2 dimer interacts with Coumarin through SH2 domains: A combined experimental and molecular modeling study

Karoline Sanches [a,b], Raphael Vinicius Rodrigues Dias [a], Paulo Henrique da Silva [a], Marcelo Andrés Fossey [a,b], Ícaro Putinhon Caruso [a,b], Fátima Pereira de Souza [a,b], Leandro Cristante de Oliveira [a], Fernando Alves de Melo [a,b,*]

[a] Department of Physics, Institute of Biosciences, Humanities and Exact Sciences, São Paulo State University "Júlio de Mesquita Filho" (UNESP), São José do Rio Preto, SP, 15054-000, Brazil

[b] Multiuser Center for Biomolecular Innovation (CMIB), Institute of Biosciences, Humanities and Exact Sciences (IBILCE), São Paulo State University "Júlio de Mesquita Filho" (UNESP), São José do Rio Preto, SP, 15054-000, Brazil

ARTICLE INFO

Keywords:
Biochemistry
Molecular biology
Biophysics
Biophysical chemistry
Spectroscopy
Biomolecules
Molecular docking
Molecular dynamics
Grb2
Coumarin
Fluorescence
STD-NMR
Molecular docking

ABSTRACT

Grb2 is an important regulator of normal vs. oncogenic cell signaling transduction. It plays a pivotal role on kinase-mediated signaling transduction by linking Receptor Tyrosine kinases to Ras/MAPK pathway which is known to bring oncogenic outcome. Coumarins are phenolic molecules found in several plants and seeds widely studied because of the antibiotic, anti-inflammatory, anticoagulant, vasodilator, and anti-tumor properties. Despite several studies about the anti-tumor properties of Coumarin in vivo and the role of Grb2 in signaling pathways related to cell proliferation, a molecular level investigation of the interaction between Grb2 and Coumarin is still missing. In this study, we performed a combined set of biophysical approaches to get insights on the interaction between Grb2 in a dimer state and Coumarin. Our results showed that Coumarin interacts with Grb2 dimer through its SH2 domain. The interaction is entropically driven, 1:1 molecular ratio and presents equilibrium constant of 10^5 M^{-1}. In fact, SH2 is a well-known domain and a versatile signaling module for drug targeting which has been reported to bind compounds that block Ras activation in vivo. Despite we don't know the biological role coming from interaction between Grb2-SH2 domain and Coumarin, it is clear that this molecule could work in the same way as a SH2 domain inhibitor in order to block the link of Receptor Tyrosine kinases to Ras/MAPK pathway.

1. Introduction

Growth factor receptor-bound protein 2 (Grb2) is an important regulator of normal vs. oncogenic cell signaling transduction [1, 2, 3, 4]. It plays a pivotal role on Fibroblast Growth Factor Receptor 2 (FGFR2) activity before extracellular stimuli by binding to it as a dimer to bring together two FGFR2 molecules in order to form a tetrameric complex 2:2 which is inhibitory for FGFR2 [5]. It also is fundamental on kinase-mediated signaling transduction by linking receptor tyrosine kinases to Ras/MAPK (mitogen-activated protein kinase) pathway which is known to bring oncogenic outcome. More recently, it was reported that the equilibrium of Grb2 monomer-dimer is determinant to its normal versus oncogenic function [6]. In that study, the authors state that Grb2 can only bind to the protein son-of-sevenless (SOS) and upregulate MAPK signaling as a monomer, but inhibits the process as a dimer [6]. Grb2 has no intrinsically enzymatic activity and it is composed of a central Src homology 2 (SH2) domain placed between two Src homology 3 (SH3) domains [7]. The SH2 domain binds to specific phosphotyrosine containing motifs on Receptor Tyrosine Kinases (RTKs) and auxiliary docking proteins [8, 9] like the insulin receptor substrates (IRSs) [5, 10, 11, 12]. On the other hand, SH3 domains are reported to recognize proline-rich motifs on several proteins including FGFR2 [13], mammalian homologue of the drosophila SOS upstream of the MAPK pathway, a guanine nucleotide exchange factor (GEF) which acts on Ras, a GTPase subfamily protein, which in turn triggers a MAP Kinase cascade and other signaling pathways [5, 12, 14, 15]. Aberrancies in the FGFR2 and MAP Kinase mediated signaling pathway are known to be involved in many human developmental pathologies and several types of cancer [14, 15, 16]. The statement of Grb2 is a regulator of those important human signaling pathways open up a new window for searching molecules with

* Corresponding author.
E-mail address: fernando.melo@unesp.br (F.A. de Melo).

https://doi.org/10.1016/j.heliyon.2019.e02869
Received 10 April 2019; Received in revised form 19 October 2019; Accepted 12 November 2019

anti-tumor properties to be characterized the interaction with Grb2 as a target protein involved in the growth of malignant cells [6].

There are several molecules with such intrinsic anti-tumor properties [17, 18, 19, 20]; among those molecules, Coumarins represent an important class of molecules that are easily found in vegetables, fruits, seeds, nuts, coffee, tea and wine. Coumarin exhibits interesting pharmacological properties that have been explored in many applications such as: antibiotic, anti-inflammatory, anticoagulant, vasodilator, anti-tumor among others [21]. The 1,2-benzopyrone is the structurally simplest member of Coumarin family and it has been reported that the treatment using this molecule showed decrease of metastatic renal carcinoma cells [22], prostatic carcinoma cells [23], breast cancer cells [24], and lung carcinoma cells [25].

Despite several studies about the anti-tumor properties of Coumarin and the role of Grb2 in signaling pathways related to cell proliferation, a molecular level investigation of the interaction between Grb2 and Coumarin is still missing. Here we present a study of the interaction between Grb2 in a dimer state and Coumarin by combining a biophysical multi-technique approach that includes Saturation Transfer Difference through Nuclear Magnetic Resonance (STD-NMR) and fluorescence experiments, molecular docking and molecular dynamics simulation. Our analysis showed that Coumarin can interact in a hydrophobic cavity placed at SH2 domain of Grb2 dimer (one per monomer). The role of this interaction is still unknown but this pocket on Grb2-SH2 domain is known to bind phosphorylated tyrosine residues on RTKs and their auxiliary docking proteins. Consequently Coumarin could somehow abrogate Grb2 interaction on cell signaling pathway mediated by RTKs in order to inhibit them.

2. Results

2.1. Binding constant and thermodynamic profile

Decrease in the fluorescence intensity can occur by several mechanisms, such as reactions with the excited state, molecular rearrangement, energy transfer, ground state complex formation, and collisional quenching [26]. The Fig. 1A shows the fluorescence emission spectra at 325 nm for Grb2 in a presence of Coumarin. Fluorescence intensity decreases while increasing Coumarin concentration in the solution, suggesting this molecule affects the micro-environment of tryptophan residues on Grb2 [26].

Grb2 concentration was set to 2 μM, which according to Lin and co-authors [5], Grb2 takes a dimer form. The maximum emission wavelength underwent a red shift up to 10 nm with the increment of Coumarin concentration. This red shift from 325 to 335 nm indicates that the polarity around the tryptophan residues involved in the interaction increases, suggesting a conformational change induced by ligand binding [26, 27]. Hence, these observations indicate that Coumarin interaction may occur in a protein region containing one or more tryptophans moderately exposed to the solvent. In order to determine the association constant for the interaction between Coumarin and Grb2, it was supposed as approach a model of two states as following [28, 29]:

$$P_f + L_f \rightarrow PL \tag{1}$$

where P_f, L_f states for free protein and free ligand in the solution, respectively, while PL states for bound protein. Assuming this model, protein-ligand association constant was calculated according to the following equation:

$$K_b = \frac{[PL]}{[P_f][L_f]} \tag{2}$$

where [PL] states for concentration of the protein-ligand complex, $[P_f]$ and $[L_f]$ states for free protein and free ligand concentrations in the solution, respectively. Rewriting [PL] to be $[P_b]$ (bound protein) and assuming that one ligand can bind to n sites of the protein, 1L → nPT (PT states for total protein concentration in the solution), it can use Scatchard equation [29] to determine K_b as following:

$$(n - \nu)K_b = \frac{\nu}{[L_f]} \tag{3}$$

where $\nu = \frac{[P_b]}{[P_T]}$ is the bound protein fraction, n is the number of ligand per protein and K_b is the association constant [30]. Scatchard plot is shown in Fig. 1B where it is possible to see a linear behavior which is characteristic for a non-cooperative binding process [26, 28]. Once K_b for each

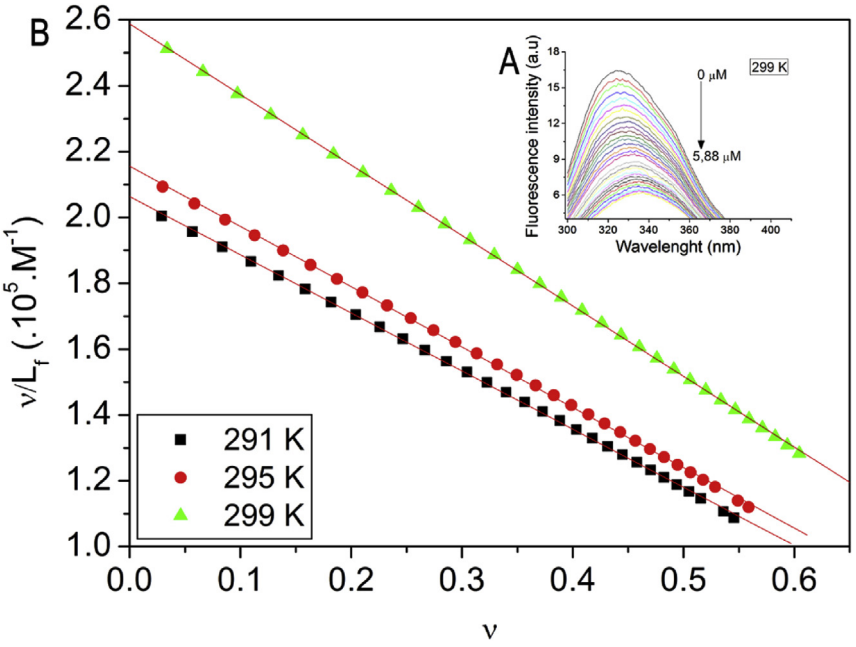

Fig. 1. (A) Emission spectra of the fluorescence intensity of Grb2 in absence and presence of increasing amount of Coumarin concentrations (from 0 to 5.88 μM). (B) Scatchard plots for the fluorescence quenching of Grb2 by the Coumarin ligand at pH 8.0 and 291 (black square), 295 (red circle) and 299K (green triangle) where K_b constant for Grb2-Coumarin interaction was calculated to be on the order of 10^5 M^{-1} assuming a 1:1 stoichiometry (n).

experimental temperature was obtained by Scatchard plot (Fig. 1B), thermodynamic profile of the Grb2-Coumarin interaction could be determined through the van't Hoff analysis (Fig. 2) by using the following equation [26]:

$$-\ln(K_b) = \frac{\Delta H}{RT} - \frac{\Delta S}{R} \quad (4)$$

where R is the universal gas constant (R = 1.98 cal.K^{-1}mol^{-1}), ΔH and ΔS are the enthalpy and entropy changes, respectively. Results for association constants, number of ligands per protein and thermodynamic parameters of interaction can be found in Table 1.

Fluorescence quenching allows the verification of the binding forces involved in protein-ligand interaction by monitoring changes of thermodynamic parameters (i.e., enthalpy change ΔH and entropy change ΔS) [26, 31, 32].

Interaction between Grb2 dimer and Coumarin was found to be favorable as Gibbs free energy decreases while increasing the experimental temperature, and entropic driven as the term TΔS is the major contribution in the thermodynamic profile of Grb2-Coumarin binding (Fig. 2B). The stoichiometry was found to be 1:1 and the association constants determined at three different temperatures were on the order of 10^5 M^{-1}, indicating a moderate interaction between Grb2 and Coumarin (Table 1).

2.2. STD-NMR spectroscopy

STD-NMR (Saturation Transfer Difference based in Nuclear Magnetic Resonance) is a powerful method for epitope mapping. This method consists in the observation of the changes in saturation of ligand specifically bound to the target protein, through the selective saturation of the protein [33, 34, 35]. Hence, based on NOE (Nuclear Overhauser effect) and changes in ligand resonance signals, STD-NMR technique allows the study of protein-ligand interaction which dissociation constants (K_D) are in a range that goes from 10^{-8} M to 10^{-3} M. The main information obtained from this technique is the ligand epitope interaction map that can be calculated through STD amplification factor by using the Eq. (5) [35, 36, 37, 38].

Table 1
Binding and thermodynamic parameters obtained from Scatchard model and van't Hoff analysis for the Grb2-Coumarin interaction at pH 8.0 and 291, 295, and 299 K. This interaction is favorable, entropycally driven within a moderate association constant (10^5 M^{-1}) and the number of ligands by protein is equal to 1. Those parameters suggest that hydrophobic effects are the major contribution on the interaction of Grb2 and Coumarin.

T (K)	Kb (10^5 M^{-1})	n	ΔG (kcal.mol^{-1})	ΔH (kcal.mol^{-1})	TΔS (kcal.mol^{-1})
291	1.7	1.0	-6.95	3.84	-10.8
295	1.8	1.1	-7.07		-10.9
299	2.1	1.2	-7.25		-11.1

$$A_{STD} = \frac{I - I_{SAT}}{I}\frac{[L_T]}{[P]} = \frac{I_{STD}}{I}\frac{[L_T]}{[P]} \quad (5)$$

where I is the signal intensity after off-resonance saturation, I_{SAT} is the intensity of on-resonance saturated signal, I_{STD} signal is the difference I-I_{SAT}, $[L_T]$ is the ligand concentration and [P] the protein concentration.

The STD effect was verified through the intensity of each Coumarin atom from the reference to difference spectra and the epitope mapping was obtaining as proportional to the STD amplification factor. The reference spectra and the difference spectra are shown in Fig. 3 in red and blue, respectively, and the results thus obtained are shown in Table 2.

The assignment ^{1}H NMR spectrum for Coumarin was done by consulting the SDBS (Spectral Database for Organic Compounds) and can be seen in the red spectrum (Fig. 3). From the epitope mapping it can be observed that the Coumarin hydrogens are surrounded by amino acid residues in the pocket of Grb2 protein when the interaction happens. Another information obtained from this approach is the spatial orientation of Coumarin in the binding site which according to the epitope mapping the hydrogens 5 and 8 are closer to the binding site in the protein, whereas these protons received more saturation transfer (Table 2). This result suggests that the benzene ring of Coumarin could be buried in the protein binding site.

2.3. Molecular docking and molecular dynamics simulations

A combined analysis of fluorescence and NMR results revealed that

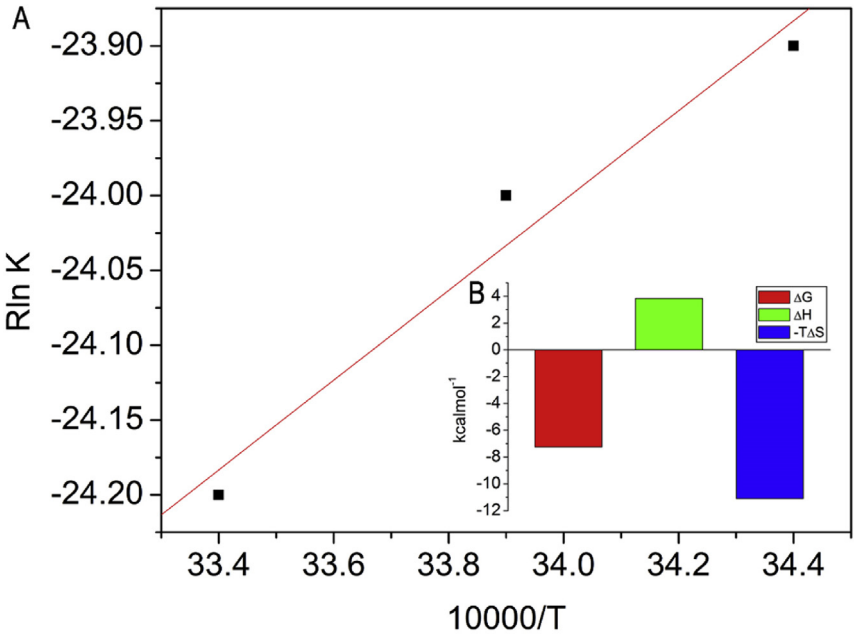

Fig. 2. (A) Van't Hoff plot and (B) thermodynamic profile showing the interaction to be spontaneous (ΔG < 0) and entropically driven (TΔS > 0) while enthalpy counts unfavorable to the interaction (ΔH > 0). This behavior is frequently associated to hydrophobic effects taking place as the major interaction mechanism [56].

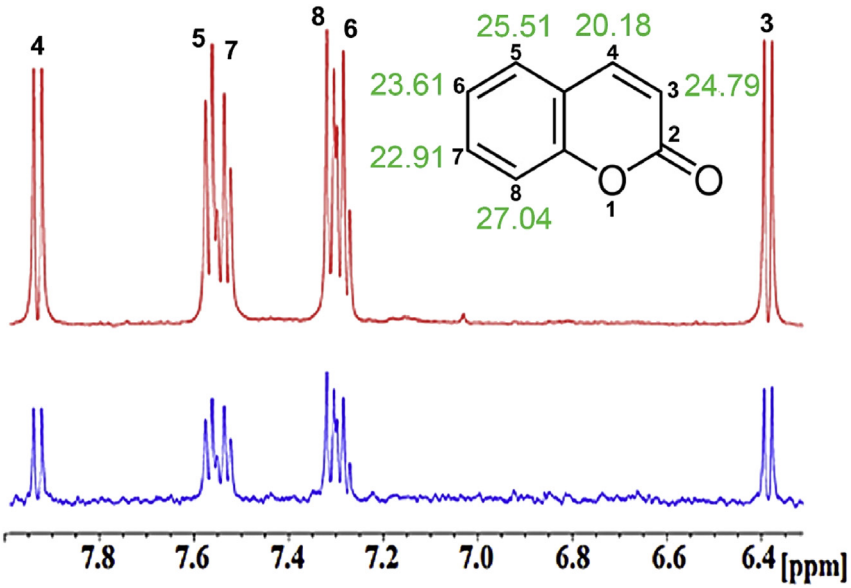

Fig. 3. Reference ^{1}H NMR of Coumarin (red) and I_{STD} spectra (blue). The signals in the I_{STD} due the saturation transfer from Grb2 to Coumarin reveals the interaction between these molecules. The STD amplification factor indicates that Coumarin is surrounded by Grb2 amino acids residues, where hydrogen atoms 5 and 8 are receiving the highest saturation transfer.

Table 2
Hydrogen position, 1D ^{1}H-NMR Coumarin chemical shift, I_{STD} and STD amplification factor. It is shown that Coumarin interacts with Grb2 in a way that hydrogen atoms 5 and 8 are the ones receiving more saturation transfer.

^{1}H	δ (ppm)	I_{STD}	A_{STD}
3	6.38	0.0925	24.79
4	7.9	0.0753	20.18
5	7.53	0.0952	25.51
6	7.28	0.0881	23.61
7	7.56	0.0855	22.91
8	7.31	0.1009	27.04

Coumarin interacts with a hydrophobic region of Grb2 containing one or more tryptophan residues. Thus, a search for the interacting region was done through molecular docking. Initially, the four largest superficial cavities were considered possible sites for this interaction and it was performed with the protein in its dimeric form (Fig. 4A) in order to match *in vitro* experimental insights with *in silico* calculations.

The search indicated four possible pockets for the ligand. However, only one was suitable with the experimental results for the interaction (Fig. 4B) located in SH2 domain of Grb2. Thus molecular docking calculations were performed using the SH2 domain and directed to the selected cavity. For statistical proposes 1500 poses were generated. The most representative conformation was selected using AMBER Score Energy and pose frequency [39] (Fig. 4C). Calculations were done considering the conformation with the lowest AMBER Score Binding Energy (as reference value) and comparing the Root Mean Square Deviation (RMSD) against all other structures. The RMSD measures the similarity between two structures and indicated 92.8% of the selected conformations with values between 0 and 1 Å (excellent agreement). Differences between 1 and 2 Å in the RMSD values were not found, 6% was found between 2 and 3 Å and only 1.2% of the values were superior to 3 Å (Fig. 5C). Those results have shown a relationship between Coumarin accessibility to different protein conformations and the interaction energy.

Since the molecular docking method used here is severely restrictive, not allowing hydration effects or side chain/ligand accommodation, was performed a molecular dynamics simulations by 20 ns using GROMACS Package [40]. The trajectories obtained from MD simulations revealed conformational changes in the protein surface, caused mainly by the movements of the side chains of the residues Ser90, Ala115, Trp121 and Arg142. These changes allow the migration of Coumarin to a more buried region of the selected pocket, resulting in the stability of the hydrophobic interaction.

Molecular dynamics trajectories from simulations were analyzed considering the energy average of short-range interactions between the protein and the ligand as comparison parameter, based on CHARMM27 force field [41]. The best conformations were selected using the lowest value of Van der Waals energy (vdw). Then, to keep an accurate energetic comparison, the complexed structure as separated in receptor and ligand, and resubmitted to the entire docking process.

The analysis showed a final value of the interaction energy obtained with AmberScore by DOCK6 of -20.62 kJ/mol. That is a lower energy value when compared to the three previous energies obtained before molecular dynamics (-13.10, -10.99, and 9.92 kJ/mol) presented in Fig. 4. Also, a more detailed analysis of the docking region has indicated Coumarin orients itself in a way that carbons are surrounded by the hydrophobic residues in from Grb2-SH2 domain pocket while oxygen atoms are faced to solvent (Fig. 5B).

The calculations indicated contacts between the Coumarin and the residues Trp121, Val88, Phe108, Leu97, His135, and Val40 (Figs. 5B and 5D) using distances less than 4 Å as the criterion of analysis. A detailed representation of the interactions can be visualized by using LIGPLOT software [42] which has revealed these six amino acids residues inside Grb2-SH2 domain pocket to hydrophobic interact with Coumarin. Arrangements of Coumarin rings with the residues Trp121 and His135 have shown a stacking-like interaction by PLIP calculations and it was included in the figure. Further analysis was performed using the MM-PBSA method [43] in which was identified the residues with highest energy contribution to the protein-ligand interaction. The result is corroborated with previous results of molecular docking, highlighting an interaction with Trp121 (Fig. 5A). Additionally, two water molecules are taking part in the interaction assembly by forming hydrogen bonds with the oxygen bound in the carbonyl of Coumarin. This interaction was calculated using the h_bond tool [44], resulting an average of 1.7 hydrogen bonds between ligand and waters during the entire trajectory.

3. Discussion

Grb2 is an important adaptor protein which is ubiquitously expressed

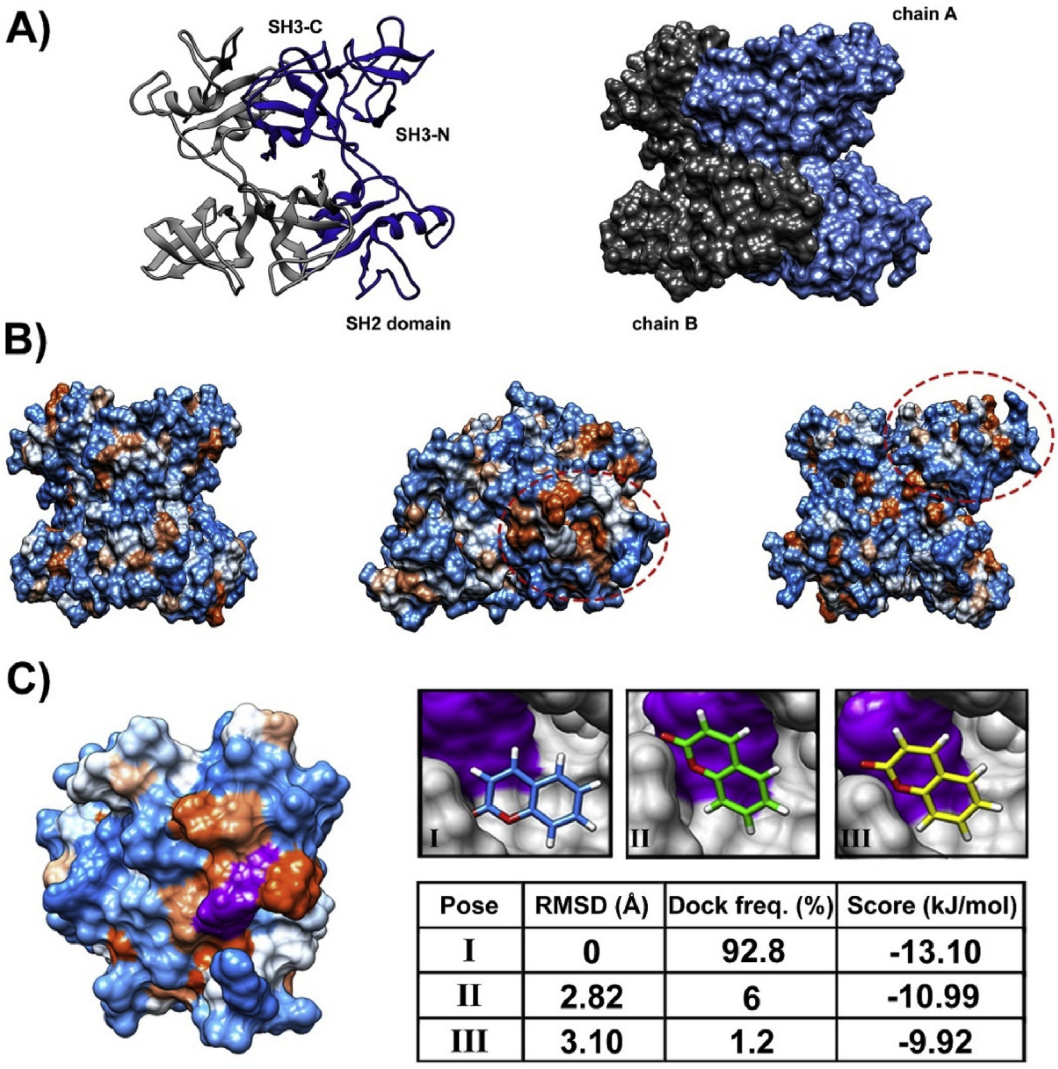

Pose	RMSD (Å)	Dock freq. (%)	Score (kJ/mol)
I	0	92.8	-13.10
II	2.82	6	-10.99
III	3.10	1.2	-9.92

Fig. 4. (A) Ribbons representation of the dimeric structure of the Grb2 protein used for computational analysis (PDBid: 1GRI). Monomers are represented in ribbons (left) and surface (right). They are distinguished in blue and gray for the chains A and B, respectively. (B) Surface representation of the Grb2 structure colored by hydrophobicity in a blue to orange scale, rotated 180° vertically twice. The SH2 domain is highlighted and presented in 3 different poses. The combined analysis of these initial attempts with the experimental results indicates only one region with reasonable accessibility, residues with similar hydrophobicity condition and presence of a tryptophan. (C) Grb2-SH2 domain surface representation employed for molecular docking calculations. The tryptophan residue is highlighted in purple and localized in the bottom of pocket (from this perspective view). This is the conformation used for Coumarin molecular docking calculations. Each pose obtained was clustered according to its RMSD and separated into three different groups, showing that the group with the highest access number (92.8%) it is also the ensemble with the lowest computational energies (around -13.10 kJ/mol).

in eukaryotic cells. It is involved in many intracellular protein interactions and readily detectable in malignant forms of breast, prostate, and colon cancers, for example. Grb2 interacts as a dimer with FGFR2 kinase and regulates its activity before extracellular stimuli [5]. Also as a dimer, it links Receptor Tyrosine Kinases signaling to Ras/MAPK pathway and regulates MAPK pathway activity through its monomer-dimer equilibrium [6]. On the other hand, Coumarins are a class of molecules presenting anti-tumor properties [17, 18, 19] which has shown efficiency on the treatment of several types of cancer cells including prostatic and breast cancer [23, 24]. But there is also a lack of information in a molecular level about them that could lead to a more efficient drug development for cancer treatment if taking Grb2 as a protein target. So, in order to characterize the interaction between Grb2 and Coumarin we have used a combination of experimental and computational analysis which started with fluorescence spectroscopy as following. Fluorescence quenching has shown the interaction between Coumarin and Grb2 dimer to be moderate with binding constant on order of $10^5 M^{-1}$ and stoichiometry 1:1 according to Scatchard Model [29]. The van't Hoff analysis have revealed interaction to be favorable as Gibbs free energy changing supports that increasing in affinity and stability are both directly proportional to the temperature increments. Raising the temperature causes a decrease in the system micro-viscosity while increasing the molecular collision due to faster diffusion which makes the interaction favorable. The calculated values for $\Delta G < 0$ are characteristic of a spontaneous reaction while $T\Delta S > 0$ indicates that entropy drives the interaction through hydrophobic effects (Fig. 2B).

The major contribution of entropy for ΔG occurs when water molecules are released from the protein solvation layer during interaction or due to protein conformational changes induced by the ligand [45]. The hydrophobic nature of Coumarin molecule also corroborates with the thermodynamic analysis. NMR-STD experiments confirmed interaction between Coumarin and Grb2. By mapping the interaction epitopes for Coumarin and Grb2, it gives us a clue of how Coumarin could dock on Grb2 binding site (Fig. 3). According to that, Coumarin is surrounded by amino acid residues during interaction with Grb2 dimer and the hydrogens 5 and 8 are receiving the highest saturation transfer (Fig. 5). Next

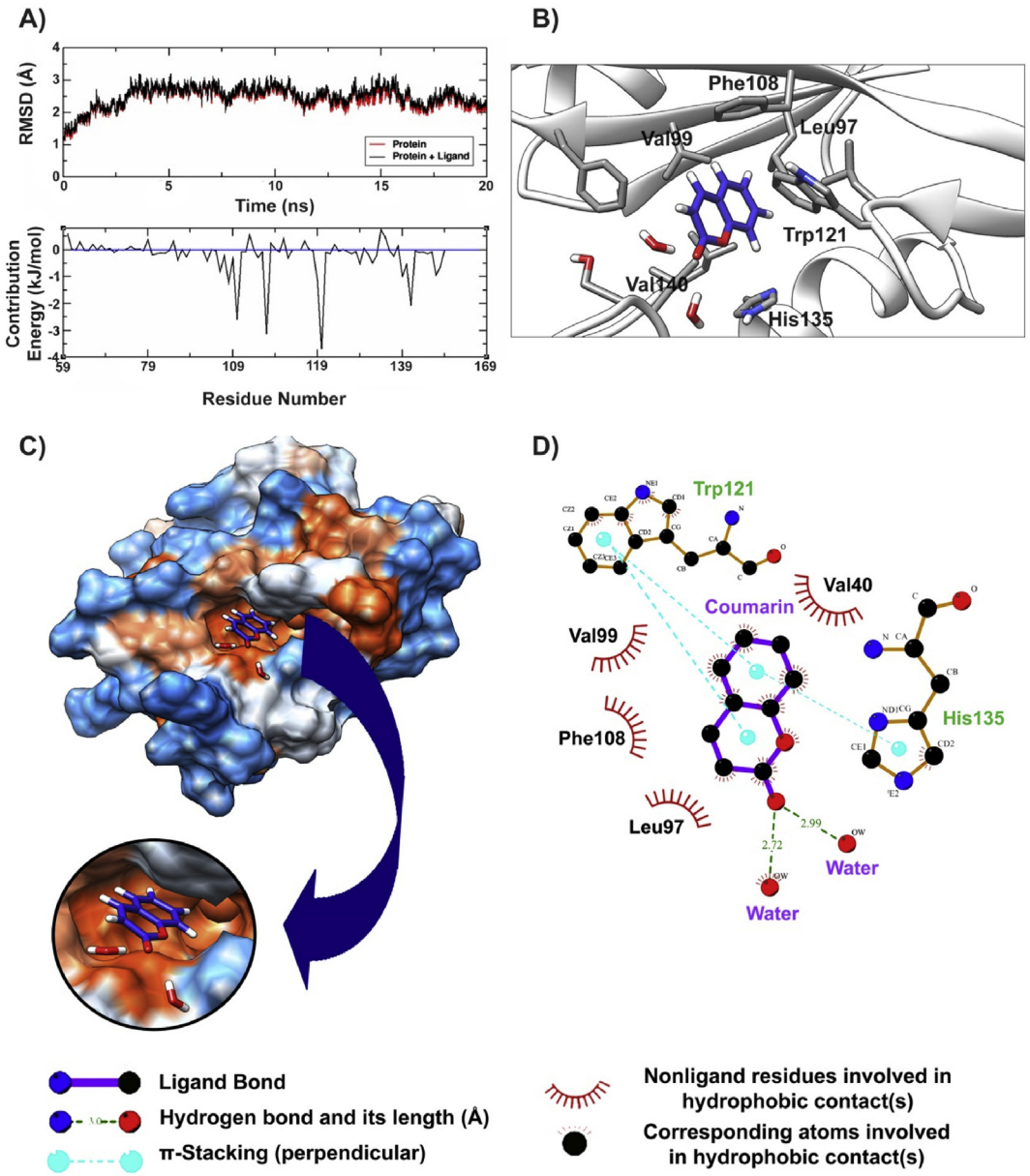

Fig. 5. Representation of the complex Grb2-Coumarin for the interaction in the Grb2-SH2 domain. (A) The upper graph is the RMSD of the protein (red) and the protein complexed with Coumarin (black) using as reference the first frame of the simulation that is the lower energy structure acquired from molecular docking. The bellow one is the energetic contribution for each residue calculated using the full molecular dynamics trajectory. For these calculations, we used the GROMACS package tools g_rms and g_mmpbsa [40, 43]. (B) Three-dimensional representation using cartoons and traces of the interaction pocket. Molecular representations were done using CHIMERA 1.7 suite [44]. (C) Grb2-SH2 domain surface representation colored by a hydrophobic scale from blue (lower) to orange (higher) with Coumarin docked in the pocket. Coumarin was colored with carbon atoms in blue, oxygen atoms in red, and hydrogen atoms in white. Water molecules taking place in the interactions are highlighted following the same patterns of nuclei. (D) Map of interactions of the complex Grb2-SH2-Coumarin. The map was obtained from two from different programs: LigPlot and PLIP. The representation was generated using LigPlot and stacking type interactions calculated by PLIP were added.

step was to employ computational simulations to determine the region on Grb2 dimer surface where Coumarin could be interacting with. In order to do that we search for a binding site which matches with experimental information as following: binding site should be hydrophobic containing one or more tryptophan residues in the bottom of it. Our computational approach found the SH2 domain on Grb2 dimer surface to be the best energy score for the interaction with Coumarin according to experimental data (Fig. 4). The binding site found in this domain is formed by hydrophobic residues and contains a tryptophan residue (Trp121) in the bottom of this cavity so in agreement with experimental data. Other places such as C-terminal Grb2-SH3 domain on the Grb2 dimer surface and Grb2 dimer interface were found which Coumarin has docked during the binding site computational search but none of than have totally matched to experimental information either by missing a tryptophan residue in cavity or by the hydrophilic nature of protein region. Besides, even Coumarin being capable of interacting with Grb2 domains separately (data not shown) by the same mechanism described here, our data suggests that Coumarin only binds to SH2 domain of Grb2 in its dimer form.

In fact, SH2 is a well-known domain and a versatile signaling module for drug targeting which has been reported to bind compounds that block Ras activation in vivo [46, 47, 48]. Despite we don't know the biological role coming from interaction between Grb2-SH2 domain and Coumarin it is clear that this molecule could work in the same way as SH2 domain inhibitors [46, 47, 48, 49] in order to block the link for Ras/MAPK signaling transduction as well. Lots of work still may be done to

understand the molecular basis which leads to cancer out come and exploring Grb2 biological role on all this process could be the way for that and for more efficient drugs development against the disease.

4. Materials and methods

4.1. Grb2 expression and purification

Grb2 protein - 6x histidine tagged - was expressed in *E. coli* BL21 (DE3) Gold. A single colony was used to transform 10 mL of LB medium which was grown for 15 h at 37 °C and shaking at 90 rpm. Then, this culture was used to inoculate 490 mL of LB containing 50 μg/mL kanamycin and 5 μg/mL tetracycline. This bacterial culture was let to shake at 37 °C until the $OD_{600} = 0.6$ being reached. After that, the temperature was lowered to 20 °C and culture was let to temperature equilibrate before induce expression by the addition of 0.4 mM IPTG. The culture was allowed to grow for a further 12 h before harvesting by centrifugation at 4000×g. The cells were re-suspended in buffer 50 mM Tris-HCl (pH 8.0) 300 mM NaCl, 1.0 mM β-mercaptoethanol (βME) in the presence protease inhibitors cocktail (Sigma Aldrich P2714-1BTL) and lysed by sonication. Cell drebis were separated by centrifugation (20,000×g at 4 °C for 45 min) and the soluble fraction was applied in metal affinity column IMAC HiTrap HP (GE Life Sciences) containing Co^{2+} ions. Following 50 mL buffer wash Grb2 was eluted with 200 mM imidazole in 50 mM Tris-HCl (pH 8.0) with 100 mM NaCl and 1.0 mM βME. The sample was concentrated to 1 mL and applied to a Superdex 75 10/300 (GE Life Sciences) gel filtration column in buffer containing 20 mM NaH_2PO_4 (pH 8.0) with 50 mM NaCl. Sample purity was confirmed by 15% SDS-PAGE to be higher than 98%.

4.2. Stock solution

The Coumarin (Sigma Aldrich) (MM 146.14 g/mol) stock solution was prepared in 90% (v/v) ethanol and kept on ice after that for up to 24 h before the interaction assays.

4.3. UV-Vis absorbance spectroscopy

UV-Vis measurements were performed on Thermo Scientific BIOMATE UV-Visible (Thermo Fisher Scientific) spectrophotometer equipped with a quartz cell of 1.0 cm path length, scanning speed of 600 nm/min, 1.0 nm of interval and spectral bandwidth of 2.0 nm. Spectra acquisition were performed at room temperature. Sample stock concentrations were obtained using the extinction coefficient of 38.055 and 11.438 $M^{-1}cm^{-1}$ for Grb2 and Coumarin, respectively [50, 51].

4.4. Fluorescence spectroscopy

Steady-state fluorescence spectroscopy measurements were performed on a spectrophotometer ISS PC1 (Champaign II, USA) equipped with a quartz cell of 1.0 cm path length and Nestlab RTE-221 thermostat bath (Thermo Electron Corporation, USA). Excitation wavelength at 290 nm was chosen since it provides excitation of tryptophan residues of protein. Emission spectrum was collected in the range of 300–500 nm, which was corrected for the background fluorescence of the buffer and for inner filter effects [26]. In the fluorescence quenching experiments performed at 291, 295, and 299 K, titrations were done by adding 2 μL from ligand stock solution (202 μM) to 2 μM Grb2 solution (2 mL) in buffer 20 mM NaH_2PO_4 (pH 8.0) with 50 mM NaCl. The final ligand concentration achieved with titrations was 5.88μM and the final ethanol concentration was 3% (v/v).

4.5. NMR spectroscopy

NMR experiments were performed on a Bruker Avance III 600.13 MHz equipped with a triple resonance 5 mm cryoprobe, having the pulse field gradient along the z axis. All data was analyzed with Bruker Topspin v3.2. Protein solution (5 μM of Grb2 in 20 mM NaH_2PO_4 buffer at pH 8.0, containing 50 mM NaCl) was used for determining the best saturation condition. It was tested at different on-resonance frequencies at -0.5, -1.0, and -1.5 ppm, keeping the off-resonance frequency at 20 ppm. Protein saturation time was reached at 3 s and recycle delay at 2 s. A total of 10 k scans were collected with 4 dummy scans. Saturation power was set to 1 ms and spinlock filter of 0.776 W was set to 1 ms at 288 K. When Coumarin was added to the system a spin lock filter of 30 ms was set for protein signals suppression. It was used 1.34 mM of Coumarin solubilized in ethanol-d6 CD_3CD_2OD (Sigma 186414).

4.6. Molecular docking and molecular dynamics simulations

Molecular docking simulations of Grb2-Coumarin complex were performed employing the tridimensional information deposited in the Protein Data Bank [52] (PDBid.: 1GRI) and the tridimensional structure of Coumarin from Compound Identification number (CID.: 323). Ligand and receptor were prepared using UCSF Chimera 1.7 [44]. Molecular docking calculations were done using UCSF Dock 6.7 package [53]. Protein cavities were identified using SPGHEN tool included in UCSF DOCK package. Throughout the docking process, the receptor Grb2 was set as rigid and the ligand as flexible initially (GRID Score step), followed by ligand and interaction receptor region flexible (AMBER rescoring). The grid box used for the ligand was divided in bins of 0.2 Å and the distance tolerance for matching ligand atoms to receptor was set to 0.75 Å. Computational docking calculation employed "anchor and grow" algorithm [54]. The first step of molecular docking was evaluated with single grid energy (SGE) score function composed by the van der Waals and the electrostatic interaction terms, also identified as Grid Score step. Then, a rescoring ranking was applied to the conformations obtained from SGE through Amber Score Binding Energy (ASBE). The calculation uses $E_{complex} = E_{binding} - (E_{receptor} - E_{ligand})$, where $E_{complex}$, $E_{receptor}$, and E_{ligand} are energies approximated by the Amber force field with MM-GB/SA method [53]. During this step small accommodations are allowed due the receptor and ligand flexibility.

Refinements of the Grb2-Coumarin complex were simulated through molecular dynamics, using as initial structure the conformation with the lowest AMBER score. The simulations were carried out using GROMACS package version 4.5.5 [40]. It was employed the force field CHARMM27 [41] with the standard set up for the protein residues and TIP3P water model. The ligand parameterization was performed using the webserver Swiss-param from Swiss Institute of Bioinformatics [55]. The MD minimization was done using 50000 steepest-descent steps and 5000 conjugate gradient steps, both without position restraints. The equilibration was performed in two steps with 100 ps, initially with and followed without position restrictions for the protein and ligand atoms. Initial atom velocities were based on Maxwell-Boltzmann distribution and the MD simulations for 20 ns with an integration step of 2 fs at 295 K, salt concentration of 0.15 M and 1 atm. The trajectory positions and energies were recorded each 100 ps. The simulation was performed using the Parrinello-Rahman barostat, Berendsen thermostat, the LYNCS method was used to constrain all hydrogen bonds and the simulation box was built with the edges of the box 10Å from the protein surface with Periodic Boundary Conditions (PBC). MD analyses were done using tools available in GROMACS package [40]. The conformation with the lowest energy of short range binding during all molecular dynamic simulation was selected, being considered the most probable conformation for the complex $Grb2_{dimeric}$-Coumarin. Since molecular simulations and docking calculations employs different energy expressions, the conformation with the lowest energy from simulations was submitted to a complete molecular docking procedure (SGE and ASBE), providing comparable energies.

Declarations

Author contribution statement

Karoline Sanches, Raphael Dias: Performed the experiments; Analyzed and interpreted the data; Wrote the paper.

Paulo Silva: Performed the experiments; Analyzed and interpreted the data.

Marcelo Fossey, Fatima Souza, Fernando Alves de Melo: Conceived and designed the experiments; Analyzed and interpreted the data; Contributed reagents, materials, analysis tools or data.

Icaro Caruso, Leandro Oliveira: Conceived and designed the experiments; Analyzed and interpreted the data.

Funding statement

This work was supported by FAPESP grant no. 2009/53989-4, 2014/17630-0, 2016/08753-6 and CNPq grant no. 442951/2014-0 and 442352/2014-0.

Competing interest statement

The authors declare no conflict of interest.

Additional information

No additional information is available for this paper.

Acknowledgements

The authors gratefully acknowledge the support of Dr. John E. Ladbury (University of Leeds, United Kingdom) for providing the Grb2 plasmid vector; Dr. Fabio R. de Moraes (Multiuser Center for Biomolecular Innovation, São Paulo State University, Brasil) for the support with the NMR data. We also thank Dr. Marcio F. Colombo (Department of Physics, São Paulo State University, Brasil) for support and for allowing us to work on the Spectroscopy Laboratory. The simulations were performed at the Center for Scientific Computing (NCC/GridUNESP) of the São Paulo State University (UNESP) and CENAPAD-SP (Centro Nacional de Processamento de Alto Desempenho em São Paulo), project UNICAMP/FINEP-MCTII.

References

[1] A.M. Tari, G. Lopez-Berestein, GRB2: a pivotal protein in signal transduction, Semin. Oncol. 28 (2001) 142–147.
[2] W. Kolch, M. Halasz, M. Granovskaya, B.N. Kholodenko, The dynamic control of signal transduction networks in cancer cells, Nat. Rev. Cancer 15 (2015) 515–527.
[3] A. Giubellino, T.R. Burke, D.P. Bottaro, Grb2 signaling in cell motility and cancer, Expert Opin. Ther. Targets 12 (2008) 1021–1033.
[4] E. Skolnik, A. Batzer, N. Li, C. Lee, E. Lowenstein, M. Mohammadi, B. Margolis, J. Schlessinger, The function of GRB2 in linking the insulin receptor to Ras signaling pathways, Science (80-) 260 (1993) 1953–1955.
[5] C.C. Lin, F.A. Melo, R. Ghosh, K.M. Suen, L.J. Stagg, J. Kirkpatrick, S.T. Arold, Z. Ahmed, J.E. Ladbury, Inhibition of basal FGF receptor signaling by dimeric Grb2, Cell 149 (2012) 1514–1524.
[6] Z. Ahmed, Z. Timsah, K.M. Suen, N.P. Cook, G.R. Lee, C.C. Lin, M. Gagea, A.A. Marti, J.E. Ladbury, Grb2 monomer-dimer equilibrium determines normal versus oncogenic function, Nat. Commun. 6 (2015) 1–9.
[7] S. Maignan, J.P. Guilloteau, N. Fromage, B. Arnoux, J. Becquart, A. Ducruix, Crystal structure of the mammalian Grb2 adaptor, Science (80-) 268 (1995) 291–293.
[8] E.J. Lowenstein, R.J. Daly, A.G. Batzer, W. Li, B. Margolis, R. Lammers, A. Ullrich, E.Y. Skolnik, D. Bar-Sagi, J. Schlessinger, The SH2 and SH3 domain-containing protein GRB2 links receptor tyrosine kinases to ras signaling, Cell 70 (1992) 431–442.
[9] K. Sanches, Í.P. Caruso, F.C.L. Almeida, F.A. Melo, NMR assignment of free 1H, 15N and 13C-Grb2-SH2 domain, Biomol. NMR Assign. (2019).
[10] G. Gorgisen, I.M. Gulacar, O.N. Ozes, The role of insulin receptor substrate (IRS) proteins in oncogenic transformation, Cell. Mol. Biol. 63 (2017) 1–5.
[11] S.R. Hubbard, The insulin receptor: both a prototypical and atypical receptor tyrosine kinase, Cold Spring Harb. Perspect. Biol. 5 (2013) a008946.
[12] M. Rozakis-Adcock, R. Fernley, J. Wade, T. Pawson, D. Bowtell, The SH2 and SH3 domains of mammalian Grb2 couple the EGF receptor to the Ras activator mSos1, Nature 363 (1993) 83–85.
[13] Z. Ahmed, C.C. Lin, K.M. Suen, F.A. Melo, J.A. Levitt, K. Suhling, J.E. Ladbury, Grb2 controls phosphorylation of FGFR2 by inhibiting receptor kinase and Shp2 phosphatase activity, J. Cell Biol. 200 (2013) 493–504.
[14] A.S. Dhillon, S. Hagan, O. Rath, W. Kolch, MAP kinase signalling pathways in cancer, Oncogene 26 (2007) 3279–3290.
[15] R.X.-D. Song, R.A. McPherson, L. Adam, Y. Bao, M. Shupnik, R. Kumar, R.J. Santen, Linkage of rapid estrogen action to MAPK activation by ERα-Shc association and Shc pathway activation, Mol. Endocrinol. 16 (2002) 116–127.
[16] I.S. Babina, N.C. Turner, Advances and challenges in targeting FGFR signalling in cancer, Nat. Rev. Cancer 17 (2017) 318–332.
[17] R. Miri, M. Nejati, L. Saso, F. Khakdan, B. Parshad, D. Mathur, V.S. Parmar, M.E. Bracke, A.K. Prasad, S.K. Sharma, O. Firuzi, Structure–activity relationship studies of 4-methylcoumarin derivatives as anticancer agents, Pharm. Biol. 54 (2016) 105–110.
[18] Y.A.-M. Abu BakarMohamad, Ahmed Al-Amiery, Abdul Amir Kadhum, Antioxidant activity of Coumarins 1 (2017) 24–30.
[19] R. Arora, S. Sawney, V. Saini, C. Steffi, M. Tiwari, D. Saluja, Esculetin induces antiproliferative and apoptotic response in pancreatic cancer cells by directly binding to KEAP1, Mol. Cancer 15 (2016) 64.
[20] V. Thomas, V. Thomas, D. Giles, D. Giles, G.P.M. Basavarajaswamy, G.P.M. Basavarajaswamy, A. Kumar Das, A. Kumar Das, A. Patel, A. Patel, Coumarin derivatives as anti-inflammatory and anticancer agents, Anti-Cancer Agents Med. Chem. Anti-Cancer Agents) 17 (2017) 415–423.
[21] S. Emami, S. Dadashpour, Current developments of coumarin-based anti-cancer agents in medicinal chemistry, Eur. J. Med. Chem. 102 (2015) 611–630.
[22] M.E. Marshall, L. Mendelsohn, K. Butler, L. Riley, J. Cantrell, C. Wiseman, R. Taylor, J.S. Macdonald, Treatment of metastatic renal cell carcinoma with coumarin (1,2-benzopyrone) and cimetidine: a pilot study, J. Clin. Oncol. 5 (1987) 862–866.
[23] J.L. Mohler, B.T. Williams, I.M. Thompson, M.E. Marshall, Coumarin (1,2-benzopyrone) for the treatment of prostatic carcinoma, J. Cancer Res. Clin. Oncol. 120 (Suppl) (1994). S35–38.
[24] M.A. Musa, J.S. Cooperwood, M.O.F. Khan, A review of coumarin derivatives in pharmacotherapy of breast cancer, Curr. Med. Chem. 15 (2008) 2664–2679. http://www.ncbi.nlm.nih.gov/pmc/articles/PMC3772644/.
[25] J.S. Lopez-Gonzalez, H. Prado-Garcia, D. Aguilar-Cazares, J.A. Molina-Guarneros, J. Morales-Fuentes, J.J. Mandoki, Apoptosis and cell cycle disturbances induced by coumarin and 7-hydroxycoumarin on human lung carcinoma cell lines, Lung Cancer 43 (2004) 275–283.
[26] J.R. Lakowicz, Principles of Fluorescence Spectroscopy, third ed., Springer, New York, 2011.
[27] J.T. Vivian, P.R. Callis, Mechanisms of tryptophan fluorescence shifts in proteins, Biophys. J. 80 (2001) 2093–2109. http://www.ncbi.nlm.nih.gov/pmc/articles/PMC1301402/.
[28] F. Ding, G. Zhao, J. Huang, Y. Sun, L. Zhang, Fluorescence spectroscopic investigation of the interaction between chloramphenicol and lysozyme, Eur. J. Med. Chem. 44 (2009) 4083–4089.
[29] F.W. Dahlquist, The meaning of Scatchard and Hill plots, Methods Enzymol. 48 (1978) 270–299.
[30] Charles R. Cantor, Paul R. Schimmel, Biophysical Chemistry - the Behavior of Biological Macromolecules, W. H. Freeman, 1971.
[31] C. Hao, G. Xu, Y. Feng, L. Lu, W. Sun, R. Sun, Fluorescence quenching study on the interaction of ferroferric oxide nanoparticles with bovine serum albumin, Spectrochim. Acta Part A Mol. Biomol. Spectrosc. 184 (2017) 191–197.
[32] A. Papadopoulou, R.J. Green, R.A. Frazier, Interaction of flavonoids with bovine serum albumin: a fluorescence quenching study, J. Agric. Food Chem. 53 (2005) 158–163.
[33] M. Mayer, B. Meyer, Group epitope mapping by saturation transfer difference NMR to identify segments of a ligand in direct contact with a protein receptor, J. Am. Chem. Soc. 123 (2001) 6108–6117.
[34] B. Meyer, T. Peters, NMR spectroscopy techniques for screening and identifying ligand binding to protein receptors, Angew. Chem. Int. Ed. 42 (2003) 864–890.
[35] A. Viegas, J. Manso, F.L. Nobrega, E.J. Cabrita, Saturation-transfer difference (STD) NMR: a simple and fast method for ligand screening and characterization of protein binding, J. Chem. Educ. 88 (2011) 990–994.
[36] M. Meyer, B. Meyer, Group Epitope Mapping by Saturation Transfer Difference NMR to Identify Segments of a Ligand in Direct Contact with a Protein Receptor, 2001. http://pubs.acs.org/doi/abs/10.1021/ja0100120.
[37] M. Mayer, B. Meyer, Characterization of ligand binding by saturation transfer difference NMR spectroscopy, Angew. Chem. Int. Ed. 38 (1999) 1784–1788.
[38] Nissler Ludwig, Rolf Gebhardt, Stefan Berger, Flavonoid Binding to a Multi-Drug-Resistance Transporter Protein: an STD-NMR Study, 2004.
[39] S.R. Brozell, S. Mukherjee, T.E. Balius, D.R. Roe, D.A. Case, R.C. Rizzo, Evaluation of DOCK 6 as a pose generation and database enrichment tool, J. Comput. Aided Mol. Des. 26 (2012) 749–773.
[40] S. Pronk, S. Páll, R. Schulz, P. Larsson, P. Bjelkmar, R. Apostolov, M.R. Shirts, J.C. Smith, P.M. Kasson, D. van der Spoel, B. Hess, E. Lindahl, GROMACS 4.5: a high-throughput and highly parallel open source molecular simulation toolkit, Bioinformatics 29 (2013) 845–854.
[41] A.D. MacKerell, D. Bashford, M. Bellott, R.L. Dunbrack, J.D. Evanseck, M.J. Field, S. Fischer, J. Gao, H. Guo, S. Ha, D. Joseph-McCarthy, L. Kuchnir, K. Kuczera, F.T.K. Lau, C. Mattos, S. Michnick, T. Ngo, D.T. Nguyen, B. Prodhom, W.E. Reiher, B. Roux, M. Schlenkrich, J.C. Smith, R. Stote, J. Straub, M. Watanabe, J. Wiórkiewicz-Kuczera, D. Yin, M. Karplus, All-atom empirical potential for

molecular modeling and dynamics studies of proteins, J. Phys. Chem. B 102 (1998) 3586–3616.
[42] A.C. Wallace, R.A. Laskowski, J.M. Thornton, LIGPLOT: a program to generate schematic diagrams of protein-ligand interactions, Protein Eng. Des. Sel. 8 (1995) 127–134.
[43] R. Kumari, R. Kumar, A. Lynn, A. Lynn, *g_mmpbsa* —a GROMACS tool for high-throughput MM-PBSA calculations, J. Chem. Inf. Model. 54 (2014) 1951–1962.
[44] E.F. Pettersen, T.D. Goddard, C.C. Huang, G.S. Couch, D.M. Greenblatt, E.C. Meng, T.E. Ferrin, UCSF Chimera—a visualization system for exploratory research and analysis, J. Comput. Chem. 25 (2004) 1605–1612.
[45] D. Leckband, J. Israelachvili, Intermolecular forces in biology, Q. Rev. Biophys. 34 (2001) 105–267. http://www.ncbi.nlm.nih.gov/pubmed/11771120. (Accessed 8 October 2019).
[46] B. Gay, S. Suarez, G. Caravatti, P. Furet, T. Meyer, J. Schoepfer, Selective GRB2 SH2 inhibitors as anti-Ras therapy, Int. J. Cancer 83 (1999) 235–241.
[47] F.-D.T. Lung, J.-Y. Tsai, Grb2 SH2 domain-binding peptide analogs as potential anticancer agents, Biopolymers 71 (2003) 132–140.
[48] K. Machida, B.J. Mayer, The SH2 domain: versatile signaling module and pharmaceutical target, Biochim. Biophys. Acta Protein Proteonomics 1747 (2005) 1–25.
[49] W.C. Shakespeare, SH2 domain inhibition: a problem solved? Curr. Opin. Chem. Biol. 5 (2001) 409–415.
[50] E. Gasteiger, C. Hoogland, A. Gattiker, S. Duvaud, M.R. Wilkins, R.D. Appel, A. Bairoch, Protein identification and analysis tools on the ExPASy server, in: J.M. Walker (Ed.), Proteomics Protoc. Handb., Humana Press, Totowa, NJ, 2005, pp. 571–607.
[51] F.P. Benzati, I.P. Caruso, T.S.P. Teixeira, F.R. Moraes, F.A. Melo, L.C. Di Stasi, M.L. Cornelio, F.P. Souza, M.A. Fossey, Investigation of the interaction between Coumarins and its derivatives with human serum albumin: STD-NMR, fluorescence and docking molecular studies, Intermt. J. Sci. 2 (2016) 1–11.
[52] F.C. Bernstein, T.F. Koetzle, G.J.B. Williams, E.F. Meyer, M.D. Brice, J.R. Rodgers, O. Kennard, T. Shimanouchi, M. Tasumi, The protein data bank: a computer-based archival file for macromolecular structures, J. Mol. Biol. 112 (1977) 535–542.
[53] P.T. Lang, S.R. Brozell, S. Mukherjee, E.F. Pettersen, E.C. Meng, V. Thomas, R.C. Rizzo, D.A. Case, T.L. James, I.D. Kuntz, DOCK 6: combining techniques to model RNA–small molecule complexes, RNA 15 (2009) 1219–1230.
[54] T.J.A. Ewing, S. Makino, A.G. Skillman, I.D. Kuntz, DOCK 4.0: search strategies for automated molecular docking of flexible molecule databases, J. Comput. Aided Mol. Des. 15 (2001) 411–428.
[55] V. Zoete, M.A. Cuendet, A. Grosdidier, O. Michielin, SwissParam: a fast force field generation tool for small organic molecules, J. Comput. Chem. 32 (2011) 2359–2368.
[56] J.E. Ladbury, M. Doyle, Biocalorimetry II: Applications of Calorimetry in the Biological Sciences, John Wiley & Sons, 2004. https://www.wiley.com/en-br/Biocalorimetry+2:+Applications+of+Calorimetry+in+the+Biological+Sciences-p-9780470849682. (Accessed 8 October 2019).